

Rigorous results on spontaneous symmetry breaking in a one-dimensional driven particle system

Stefan Großkinsky, Günter M. Schutz^Y, Richard D. Williams^Y

December 29, 2021

Abstract

We study spontaneous symmetry breaking in a one-dimensional driven two-species stochastic cellular automaton with parallel sublattice update and open boundaries. The dynamics are symmetric with respect to interchange of particles. Starting from an empty initial lattice, the system enters a symmetry broken state after some time T_1 through an amplification loop of initial fluctuations. It remains in the symmetry broken state for a time T_2 through a trapping mechanism. Applying a simple martingale argument, we obtain rigorous asymptotic estimates for the expected times $\langle T_1 \rangle \sim L \ln L$ and $\ln \langle T_2 \rangle \sim L$, where L is the system size. The actual value of T_1 depends strongly on the initial fluctuation in the amplification loop. Numerical simulations suggest that T_2 is exponentially distributed with a mean that grows exponentially in system size. For the phase transition line we argue and confirm by simulations that the flipping time between sign changes of the difference of particle numbers approaches an algebraic distribution as the system size tends to infinity.

Keywords. spontaneous symmetry breaking, bridge model, cellular automaton, two-component exclusion process, martingale

1 Introduction

Spontaneous symmetry breaking (SSB) is associated with phase transitions and is therefore not expected at positive temperature in one-dimensional

Statistical Laboratory, University of Cambridge, Cambridge CB3 0W B, UK
email: stefan@statslab.cam.ac.uk, phone: +44 1223 337962

^YInstitut für Festkörperforschung, Forschungszentrum Jülich, 52425 Jülich, Germany

equilibrium system with short-range interactions. The underlying physical picture behind the absence of 1-d phase transitions, viz. the unsuppressed creation of islands of the minority phase inside a region of the majority phase (e.g. in an Ising system) due to thermal noise, is very robust. So it came as a bit of a surprise that in a quite simple stochastic (and hence noisy) lattice model of a driven diffusive system with short-range interactions SSB was observed [1, 2]. In this so-called bridge model, two species of particles A;B move in opposite directions with rate 1 and are injected with rate α and ejected with rate β at the boundary sites. Although the dynamical rules are symmetric with respect to the two species, two phases with non-symmetrical steady states were found in a mean-field approximation. In the symmetry broken states there is a macroscopic excess amount of one particle species, i.e., the order parameter $\rho_A - \rho_B$ measuring the difference of the average particle densities of the two species A;B attains a non-zero value in the thermodynamic limit $L \rightarrow \infty$. These analytical results were confirmed by Monte Carlo simulations of finite systems of large size L .

In the limit of vanishing ejection rate ($\beta \rightarrow 0$) the existence of SSB in this model could be established rigorously [3]. It emerged that (at least in this limit) the phases of spontaneously broken symmetry are dynamically sustained by a traffic jam effect: The particles of one species pile up at one end of the chain (because of the small rate of ejection) and thus prevent the entrance of particles of the other species, until by an exponentially rare fluctuation (i.e. with a probability exponentially small in system size) no particles of that species enter for sufficiently long time. Then the traffic jam dissolves, allowing for particles of the other species to take over. Later some other stochastic 1-d lattice gas models exhibiting SSB were discovered [4, 5], but the nature of the phase transition in the bridge model has remained obscure [6, 7]. There is, in fact, recent numerical evidence suggesting that one of the two symmetry broken phases vanishes in the thermodynamic limit [8, 9].

It would seem natural to attack the problem of SSB from a macroscopic viewpoint by deriving a hydrodynamic description of the lattice gas model under Eulerian scaling. This approach indeed works for vanishing boundary rates [10], but fails for the general case due to the lack of a sufficiently general hydrodynamic theory for two-component systems in the presence of boundaries [11]. Only partial results for some specific finite multi-component systems are known [12, 13, 14, 15, 16, 17].

These and other puzzles make driven diffusive two-component systems a matter of considerable current interest, see [18] for a review. In [19] we studied a variation of the bridge model with parallel sublattice update. The deterministic bulk update scheme simplifies the treatment of particle transport, while stochastic creation/annihilation events occur at the

boundaries in a similar fashion as in the original bridge model. Thus { while maintaining noisy dynamics { the complexity of the problem is reduced. This allowed us to determine the exact phase diagram (for all values of the boundary rates) and to elucidate the mechanism that leads from a symmetric particle configuration into a state with broken symmetry. In this work we make rigorous the main results reported in [19], which are complemented by new heuristic results on the transition line. We also point out that earlier work on a similar single-component system [20] yields a rigorous asymptotic estimate for the residence time in a symmetry broken quasi-stationary state of the two-component system and we present new results on the phase transition between the symmetric and the symmetry broken phase.

In Sec. 2 we define the model and state our main results for the symmetry broken phase. The proofs are given in Sec. 3. In Sec. 4 we present simulation data which provide further insight in the relevant time scales of the model. Analytical and simulation results for the phase transition line are given in Sec. 5. We conclude in Sec. 6 with some brief remarks.

2 Model and results

2.1 Bridge model with sublattice parallel update

The model considered here is defined on a one-dimensional lattice of length L , where L is an even number. Sites are either empty or occupied by a single particle of either species A or B, i.e., the particles are subject to an exclusion interaction and the occupation numbers $n_A(i)$ and $n_B(i)$ of each site i obey $n_A(i) + n_B(i) \leq 1$. The dynamics is defined as a parallel sublattice update scheme in two half steps. In the first half-step the following processes take place: At site 1 it is attempted to create a particle of species A with probability $\frac{1}{2} [0;1]$ if the site is empty, or to annihilate a particle of species B with probability $\frac{1}{2} [0;1]$, provided the site is occupied by such a particle:

$$0 \rightarrow A ; B \rightarrow 0 : \quad (1)$$

Accordingly, at site L a particle of species B is created with probability $\frac{1}{2}$ and a particle of species A is annihilated with probability $\frac{1}{2}$:

$$0 \rightarrow B ; A \rightarrow 0 : \quad (2)$$

In the bulk, the following hopping processes occur deterministically between sites $2i$ and $2i+1$ with $0 < i < L/2$:

$$A0 \rightarrow 0A ; 0B \rightarrow B0 ; AB \rightarrow BA : \quad (3)$$

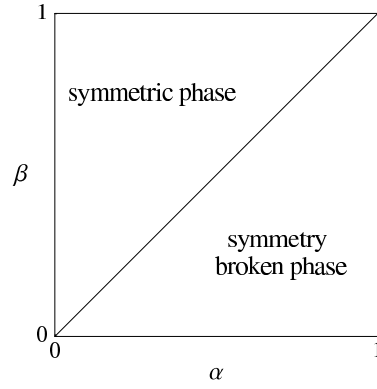


Figure 1: Stationary phase diagram of the sublattice bridge model as a function of creation and annihilation probabilities α and β .

In the second half-step, these deterministic hopping processes take place between sites $2i-1$ and $2i$ with $0 < i \leq L/2$. Note that the dynamics is symmetric with respect to interchange of the two particles species combined with space reflection. The original bridge model [1, 2] arises as the continuous-time limit of this model with stochastic hopping and has the same symmetry.

2.2 Results

The stationary phase diagram of the model in terms of the parameters α and β is presented in Figure 1. The boundary lines are not difficult to analyze. Along the line $\beta = 0; 0 < \alpha < 1$ there is no injection and the stationary state is the empty lattice (which is trivially symmetric in A and B). For $\alpha = 1; 0 < \beta < 1$ it is easy to verify by direct computation that the product measure with alternating densities $\rho_A(i) = 0, \rho_B(i) = \beta/(1+\beta)$ if i is odd, and $\rho_A(i) = \beta/(1+\beta), \rho_B(i) = 0$ if i is even is invariant. Also this stationary state is symmetric. For $\alpha = 0; 0 < \beta < 1$ there is no ejection and the system is highly non-ergodic. Any blocking measure with A-particles accumulating at the right boundary and B-particles accumulating at the left boundary is invariant. We notice that most of these measures are not symmetric. Finally, for $\alpha = 1; 0 < \beta < 1$ there are two stationary product measures, one with $\rho_B(i) = 0$ for all i and $\rho_A(i) = 1$ for even $i, \rho_A(i) = 0$ for odd i and an analogous one with A and B particles interchanged. In each case one species is completely expelled from the system even on a finite lattice. This is a trivial, absorbing form of SSB with no transition between the two states. The dynamics reduce to that of the single-species

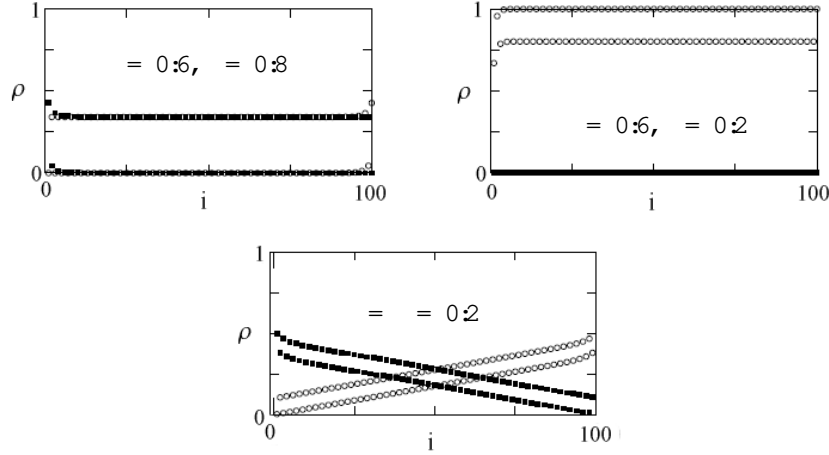


Figure 2: Average density profiles obtained from Monte Carlo simulations in the symmetric phase (top left), the broken phase (top right) and on the transition line (bottom). A densities are shown by \circ , B densities by \bullet .

lattice gas studied by one of us earlier [20]. In the special deterministic point $\alpha = \beta = 1$ there are three invariant measures arising as limits of the measures described above. One is the symmetric alternating $A=B$ measure ($\alpha = 1; \beta = 1$), the other two are the symmetry-broken measures with only A or only B particles ($\alpha = 1; \beta = 0$ and $\alpha = 0; \beta = 1$). These considerations hold for all system sizes L , and in what follows the boundary lines are excluded from the discussion.

The interior of the phase diagram can be explored by Monte Carlo simulations [19]. Two phases are found:

If $\alpha < \beta$, the system exhibits a symmetric steady state. Here, the bulk densities in the limit $L \rightarrow \infty$ are $\rho_A(i) = 0$, $\rho_B(i) = \frac{\alpha}{\alpha + \beta}$ if i is odd, and $\rho_A(i) = \frac{\alpha}{\alpha + \beta}$, $\rho_B(i) = 0$ if i is even.

If $\alpha > \beta$, the system resides in the symmetry broken phase. Assume the A particles to be in the majority. Then, the bulk densities in the limit $L \rightarrow \infty$ are $\rho_B(i) = 0$ for all i , $\rho_A(i) = 1$ for i even and $\rho_A(i) = 0$ for i odd. This means that the symmetry is maximally broken and the minority species is completely expelled from the system.

On the transition line for $\alpha = \beta$ the system switches between symmetric and broken states, which is studied numerically in Section 5.

The intention of this paper is to further elucidate the dynamics leading to symmetry breaking which were identified in [19] and to determine rigorously the time scales associated with SSB for $\gamma > \gamma_c$.

If one of the species is expelled from the system, the dynamics of the majority species for $\gamma > \gamma_c$ is identical to the single species ASEP with parallel sublattice update. The exact steady state distribution for this system has been characterized in [20] for all γ , and all system sizes L . Let μ_0 be the distribution that concentrates on the empty lattice for the single species system. Then we write

$$\mu_A = \mu_0 \quad \text{and} \quad \mu_B = \mu_0 \quad (4)$$

for the distributions of our two species system, where one of the species is expelled and the other distributed according to μ_0 . Note that we do not explicitly write the dependence of μ_A and μ_B on γ , and L . We say that the system reaches a configuration $\sigma = (\sigma_A(i); \sigma_B(i))_{i=1, \dots, L}$ with broken symmetry if $\sigma_A(i) = 1$ for all even i and $\sigma_B(i) = 0$ for all i , or vice versa $\sigma_B(i) = 1$ for all odd i and $\sigma_A(i) = 0$ for all i . Let $T_1(\sigma)$ be the (random) time when the system first reaches a symmetry broken configuration, starting from configuration σ . $T_2(\sigma)$ is defined to be the time until the first particle of species B enters the system. With these definitions we can state the main results of this paper.

Theorem 1 Time to reach a symmetry broken configuration

$$\text{For } \gamma > \gamma_c \text{ we have } \limsup_{L \rightarrow \infty} \frac{\mathbb{E} T_1 \mu_0}{L \ln L} < 1.$$

Here $\mathbb{E} \cdot$ denotes the expected value over the time evolution of the process with initial distribution μ_0 . So if we start the process with an empty lattice ($\mu_0 = \mu_0$) then the expected time to reach a symmetry broken state is not growing faster than $L \ln L$ with the system size L .

Theorem 2 Stability of states with broken symmetry

$$\text{For } \gamma > \gamma_c \text{ we have } \liminf_{L \rightarrow \infty} \frac{\mathbb{E} T_2 \mu_A}{L} > 0.$$

So starting with a symmetry broken state μ_A where the B particles are expelled from the system, the expected time until the next B particle enters grows exponentially with L . By symmetry an analogous statement holds if A and B particles are interchanged.

Since $\mu_A = \mu_0$ and μ_0 is stationary for the single species system, μ_A is invariant for the two species system for times $t < T_2$. So although μ_A and μ_B are not stationary for finite L , they are exponentially stable

by Theorem 2 for $\beta > \beta_c$. Together with Theorem 1 this provides a proof for spontaneous symmetry breaking in this model in the interior region of the phase diagram. Note that this argument is done without knowing the stationary distribution exactly, which should of course be close to the mixture $\frac{1}{2} \rho_A + \frac{1}{2} \rho_B$, corresponding to the usual concept of a phase transition in the context of Gibbs measures (e.g. in an Ising system).

The proofs are given in Section 3, where the proof of Theorem 2 is a straightforward application of the results in [20]. The proof of Theorem 1 relies on a simple martingale argument for an interesting amplification mechanism which has been published in [19], and will be explained again in the next subsection for self-containedness.

2.3 Dynamics of symmetry breaking

It is assumed that at $t = 0$ there are no particles in the system and that $\rho_A > \rho_B > 0$. Other symmetric initial conditions with a non-empty lattice can be treated in a similar fashion. Starting from the empty lattice, A (B) particles are created at every time step with probability ρ_A (ρ_B) at site 1 (L). Once injected, particles move deterministically with velocity 2 (-2). Therefore, at time $t = L/2$ the system is in a state where the density of A (B) particles is ρ_A (ρ_B) at all even sites and 0 (ρ_B) at all odd sites. In this situation both creation and annihilation of particles are possible.

However, it turns out that the effect of creation of particles is negligible: Since $\rho_A > \rho_B$ the deterministic hopping with velocity 2 transports on average more A-particles towards site L than can be annihilated there. This leads to the formation of an A-particle jam at the right boundary, blocking the injection of B-particles. An analogous argument holds for the left boundary, which is blocked by a B-particle jam. In these jams, the only source of vacancies is annihilation at the boundaries with probability ρ_B in the first half-step. In the second half-step the vacancy moves one site towards the bulk with probability 1. Therefore, in a jam, the density of A (B) particles at even (odd) sites is 1, while that at odd (even) sites is 0. So the only way to create particles in this situation is a complete dissolution of a jam. But as long as it gains particles from transport through the bulk this is a very rare event since $\rho_A > \rho_B$. We show in Lemma 3.2 (Section 3) that the average number of created particles is small and bounded independent of L . So creation of particles in this jammed situation becomes negligible in the limit $L \rightarrow \infty$ and will be neglected in the following explanation.

The number of particles in each of the two jams reduces by one in every time step with probability ρ_B . Since creation of particles is negligible, the influx into the jam ceases after some time and the jam eventually dissolves. By fluctuations, one of the jams, say the B-jam at the left boundary, dissolves first. A particles can enter the system while B particles

are still blocked until the A-jam at the right boundary is also dissolved. The configuration of the system at this point is illustrated in Figure 3 at time t_1 (setting $k = 1$). The light grey region denotes a region of low density of A particles where the density is 0 on even (odd) sites. The (random) length of this region, ℓ_1 , describes the majority of one of the species. The description is symmetric, so if $\ell_1 < 0$ this corresponds to a majority of B particles. Thus the average value $\langle \ell_1 \rangle_0 = 0$, but typically $\ell_1 = O(\sqrt{L})$ due to fluctuations for large L and one of the species has the majority (see Lemma 3.3 in Section 3).

The time evolution just described constitutes the first cycle of a periodic behavior which can be effectively described by the dynamics of low density regions and jams at the boundaries. The key ingredient for this simplification is the jamming mechanism described above. The cyclic behavior consists of 4 stages, which we summarize in the following and which are illustrated in Figure 3. For simplicity of presentation we assume that $\ell_k \geq 0$, i.e. the A particles have the majority.

1. At the beginning of a cycle ($t_1 = 0$) there is a low density region of A particles at the left boundary of length $j \ell_k \geq 0$.

Both species enter the system with probability $\frac{1}{2}$ and penetrate the bulk deterministically with speed $2(1-\alpha)$.

2. The low density region of A particles reaches the right boundary at time $t_2 = L - j \ell_k = 2$, blocking the creation of B particles.

A particles still enter with probability $\frac{1}{2}$ and exit with probability $< \frac{1}{2}$, further increasing their majority.

3. At time $t_3 = L=2$ the B particles reach the left boundary, blocking also the creation of A particles.

Both species form jams at the boundaries, which gain particles from the low density regions. Since creation of particles at the boundaries is negligible, both jams eventually dissolve.

4. Let t_4 be the time when the jam of B particles is dissolved.

A particles start to enter the system. Again, since $\ell_k > 0$ the majority of A particles increases on average.

5. At time t_5 the A-jam at the right boundary is dissolved and also B particles can enter the system.

The cycle is finished when both jams are dissolved, i.e. at time $\max\{t_4, t_5\}$. Note that for given ℓ_k, t_1, t_2 and t_3 are deterministic, whereas t_4 and t_5 are random times, which will be defined more precisely in Section 3. In

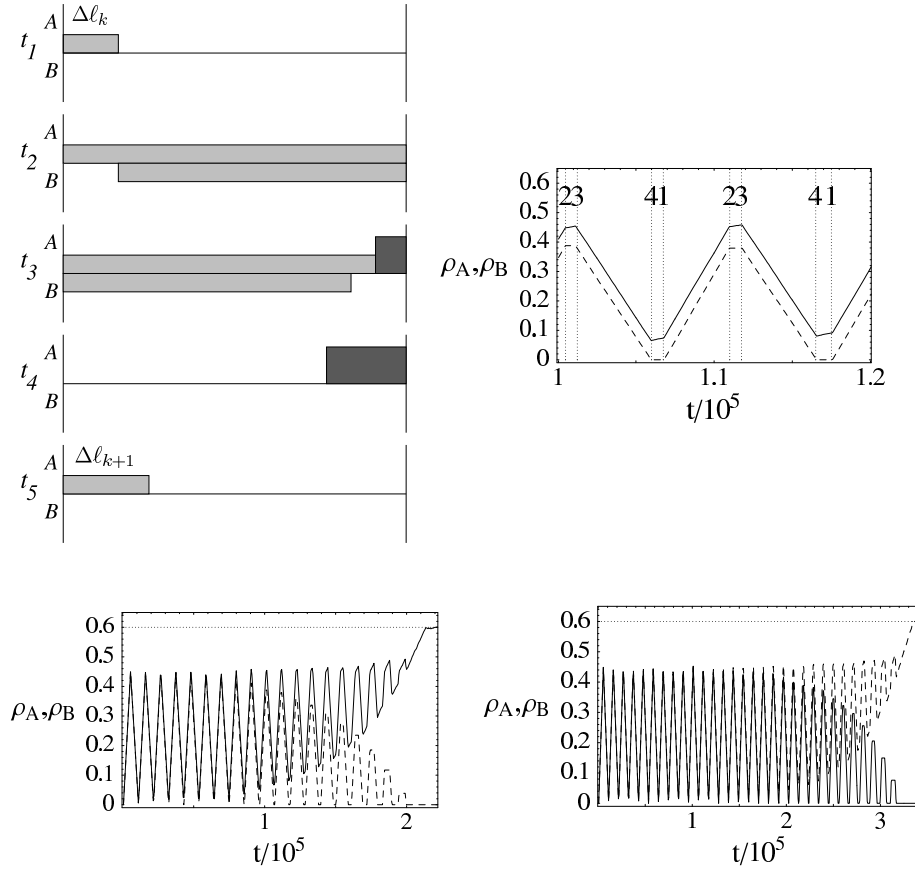


Figure 3: Cyclic behavior of the dynamics of symmetry breaking.
Top: Illustration of the stages involved in the k -th cycle of the amplification loop as explained in the text. Low density regions are drawn light grey, jams are dark grey and white regions of the system are empty. On the right the stages are identified in a blow-up of simulation data shown in the bottom.
Bottom: Two realizations of M C simulation of symmetry breaking, starting from the empty lattice with $\rho_A = 0.9$, $\rho_B = 0.8$ and $L = 10000$. The density ρ_A is drawn in a full line ($|$), ρ_B in dashed line ($--$) and the dotted line indicates the density in the symmetry broken state.

Figure 3 it is assumed that the B-jam dissolves first, i.e. $t_4 < t_5$, which is most likely if $\ell_k > 0$. But in general $t_4 > t_5$ is also possible and included in the above description. The result of the cycle is

$$\ell_{k+1} := 2(t_5 - t_4); \quad (5)$$

which is the initial condition for the next cycle. As long as $L < \ell_{k+1} < L$ the cycle can restart with $0 < t_2 < t_3$, and all the stages are well defined. Note that within this framework the process starting from the empty lattice is a cycle with initial condition $\ell_0 = 0$ and $t_2 = t_3$. The cyclic behavior leads to an amplification of the initial fluctuation ℓ_1 , namely

$$\ln \ell_k / \ln \ell_0 \sim 2^k \quad \text{for large } L; \quad (6)$$

as given in Lemma 3.2. Together with the fact that the average duration of a cycle is of order L (see Lemma 3.3), this is the core of the proof of Theorem 1 provided in the next subsection.

3 Proofs

3.1 Proof of Theorem 1

In order to define the random times t_4 and t_5 in the cycle described above more precisely, we use the following procedure: At time t_2 we mark the last particle of the minority species, corresponding to the rightmost B particle in the above description. If due to a fluctuation there is no particle of that species in the system, the cycle is finished at t_2 with $\ell_{k+1} = L$ and also the amplification loop stops. Otherwise, we analogously mark the last particle of the majority species at time t_3 and define t_4 and t_5 to be the time when the marked B and A particle, respectively, just left the system. If there were no particles of the majority species in the system at time t_3 , we set $t_5 = t_3$ (or $t_4 = t_3$ if the B particles have the majority). At time $\max(t_4, t_5)$ we restart the cycle with initial condition ℓ_{k+1} given in (5). This determines a process $(\ell_k)_{k=0,1,\dots}$ on \mathbb{Z} with $\ell_0 = 0$. If $j \ell_{k+1} \leq L$ the process stops and we reach a symmetry broken state.

We first note some Lemma's used in the proof. The proofs of the Lemma's are given in the next subsection.

Lemma 3.1 If $j \ell_k \leq L$ the system reaches a symmetry broken configuration as defined in Section 2.2 within a time of order L .

We define k to be the (random) number of cycles performed when the loop stops, i.e.

$$k := \inf \{k : j \ell_k \leq L\}; \quad (7)$$

This is a stopping time for the process $(\tau_k)_{k=0;1;\dots}$ and in the following we aim to find an estimate on the expected value $h\tau_k$. We will use the following recursion relation:

Lemma 3.2 For a single cycle

$$\tau_{k+1} - \tau_k = q \tau_k + C_k; \quad (8)$$

where $q = 2 - \frac{1}{L} > 1$ and the constants C_k are bounded independent of L and k . This constitutes an amplification of the initial fluctuations τ_1 and we get inductively

$$\tau_{k+1} - \tau_1 = q^k \tau_1 + \sum_{i=1}^k C_i q^{k-i}; \quad (9)$$

Here and in the following we omit the subscript 0 since all expectations are understood with respect to the empty initial condition.

Lemma 3.3 The average length of a cycle is bounded above by

$$h\tau_j | \tau_1 = i = -1 + \frac{L}{2} + \sum_{k=1}^{\infty} q^k (\tau_k - \tau_1) = 2 = O(L); \quad (10)$$

and the initial fluctuation is of order $\frac{1}{L}$ since

$$\text{Var}(\tau_1) = 4L \frac{(2 - \frac{1}{L})}{2}; \quad (11)$$

To get an estimate for $h\tau_k$ we use the optional stopping theorem for martingales. Since $q > 1$ and $\tau_1 = O(\frac{1}{L})$ as shown in (11), it is clear from (8) that $(\tau_k)_k$ is a sub-martingale for sufficiently large L . Conditioned on the initial value τ_1 we define the process $(Y_k)_{k=1;2;\dots}$ by $Y_1 = \tau_1$ and

$$Y_k - Y_{k-1} = \tau_k - \tau_{k-1} \quad \text{for } k \geq 2; \quad (12)$$

following Doob's decomposition of sub-martingales. By construction, $(Y_k)_k$ is a martingale and k is a stopping time for $(Y_k)_k$. Thus by optional stopping and using Lemma 3.2 we have for $k \geq 2$

$$\begin{aligned} 0 &= hY_k | \tau_1 = i - hY_{k-1} | \tau_1 = i \\ &= h\tau_k | \tau_1 = i - q h\tau_{k-1} | \tau_1 = i - hC_{k-1} | \tau_1 = i; \end{aligned} \quad (13)$$

Also by Lemma 3.2 we know that $h\tau_k | \tau_1 = i = qL + O(1)$, since otherwise, the process would have stopped before k . Using (9) and $hC_{k-1} | \tau_1 = i = O(1)$ we get

$$qL + O(1) - q h\tau_{k-1} | \tau_1 = i = -h\tau_1 + O(1) hq^{k-1} | \tau_1 = i; \quad (14)$$

Since $q > 1$ Jensen's inequality yields

$$q^{h_{kj} \cdot 1} = h_{kj} \cdot 1 \leq q \frac{qL + O(1)}{q \cdot 1 + O(1)} : \quad (15)$$

This leads to

$$h_{kj} \cdot 1 \leq 2 + \frac{\ln L = j \cdot 1 + o(1)}{\ln q} : \quad (16)$$

Again with Jensen's inequality we have

$$\ln L = j \cdot 1 \leq \ln L h_{1j} \quad (17)$$

Since with Lemma 3.3, $1 = j \cdot 1 = O(L^{-1/2})$ we get

$$h_{ki} \leq O(1) + \frac{\ln L}{2 \ln q} (1 + o(1)) : \quad (18)$$

Therefore, taking the expected value w.r.t. $\cdot 1$, the expected total time spent in the amplification loop is of order $L \ln L$. Together with Lemma 3.1 this finishes the proof.

3.2 Proof of Lemma 3

Proof of Lemma 3.2. In the following we analyze the distributions of the random variables t_4 and t_5 to get the time evolution of \cdot_k . Let τ_n be the (random) time it takes for a jam of n particles to dissolve. With this

$$t_4 = L = 2 + N_B + E_B^k ; \quad t_5 = L \cdot \cdot_k = 2 + N_A + E_A^k : \quad (19)$$

Here N_A (N_B) denotes the number of A (B) particles that entered the system up to time t_3 (t_2) before blocking, including \cdot_k . E_A (E_B) denotes the number of time steps where the A (B) jam is dissolved, i.e. site $L(1)$ is empty before t_4 (t_5), when the respective marked particle exits. These are fluctuations and may lead to single B (A) particles that enter the system due to lack of blockage. We call such particles discrepancies and below we show that their expected number is bounded independent of the system size L . Apart from that, the boundary site in a jam is always occupied and particles are annihilated with probability \cdot . So the time $\tau_{1/2} \dots \tau$ for one particle to leave the jam is a $\text{Geo}(\cdot)$ geometric random variable with

$$P(\tau = k) = (1 - \cdot)^{k-1} ; \quad h_{ii} = 1 - \cdot : \quad (20)$$

Let τ_i for $i = 1, \dots, n$ be n independent copies of τ and $n \geq N$ an independent random variable. Then for

$$\tau_n = \sum_{i=1}^n \tau_i \quad \text{we have} \quad h_{\tau_n} = \ln h_{\tau} = \ln(1 - \cdot) : \quad (21)$$

In (19) $n = N_A$ or N_B is a $\text{Bi}(t; \cdot)$ binomial random variable with

$$P_{n=k} = \binom{t}{k} (1-p)^{t-k} p^k; \quad k=0, \dots, t; \quad \text{hni} = t: \quad (22)$$

For $n = N_A$ it is $t = \tau_k = 2 + t_3 - B_A^k$ and for $n = N_B$, $t = t_2 - B_B^k$, where B_A (B_B) is the number of time steps where the entrance of A (B) is blocked by singular B (A) discrepancies. With (22) we have

$$\begin{aligned} \text{h}N_A^k &= \tau_k = 2 + t_3 - B_A^k = L + \tau_k = 2 - B_A^k; \\ \text{h}N_B^k &= t_2 - B_B^k = L - \tau_k = 2 - B_B^k; \end{aligned} \quad (23)$$

where all expected values are conditioned on τ_k . According to (20), dividing (23) by τ_k yields $\text{h}N_A^k$ and $\text{h}N_B^k$. Using this and (23) the average value of $\tau_{k+1} = 2(t_5 - t_4)$ conditioned on τ_k is given by

$$\tau_{k+1} - \tau_k = 2 - 1 - \tau_k + 2\text{h}E_A^k - E_B^k - 2 - B_A^k - B_B^k: \quad (24)$$

This is equal to (8) with

$$C_k = 2\text{h}E_A^k - E_B^k - 2 - B_A^k - B_B^k = 2\text{h}E_A^k - E_B^k - 2\frac{1}{2}\text{h}E_A^{k-1} - E_B^{k-1} \quad (25)$$

since the blocking of A particles is caused by discrepancies of the previous cycle, i.e. $B_A^k = -E_A^{k-1}$ and analogous for B particles. (9) follows directly by induction.

In order to finish the proof it suffices to show that $\text{h}E_A^k$ and $\text{h}E_B^k$ are bounded independent of L for all k . Recall that an A-jam is defined as a region of A particles at the right boundary with densities 1 on even and 1/2 on odd sides. Denote by M_t , $t \geq t_2$, the number of particles in the A-jam at time t . If $M_t > 0$ it decreases by 1 with probability $1/2$ in each time step. Until the marked A particle reaches the jam, say at time $t(L)$, M_t increases at least by 1 with probability $1/2$ in each time step. Due to the sublattice parallel update, also an increase by two particles is possible. Both statements are true only modulo finite corrections due to discrepancies. Nevertheless, M_t performs a biased random walk and is increasing on average. Thus it visits 0 only finitely often for $t \rightarrow \infty$, and thus also for $t \leq t(L)$. Now

$$E_A^k = \mathbb{E}[M_{t_2+t(L)}] : M_{t_2} = 0; \quad (26)$$

and thus $\text{h}E_A^k$ is bounded independent of L . The same argument holds for $\text{h}E_B^k$, finishing the proof.

Proof of Lemma 3.3. With (19) and (23) we have

$$h t_5 i = L \left(h \rho_k i = 2 + \frac{1}{L} + h \rho_k i \right) = (2 + \frac{1}{L}) \left(h B_A^k i + h E_A^k i \right); \quad (27)$$

where all the expected values are conditioned on ρ_1 . This leads directly to (10).

In the initial cycle starting with the empty lattice, t_4 and t_5 are iid.r.v's and thus with $\rho_1 = 2(t_5 - t_4)$ we get

$$\text{Var}(\rho_1) = 4 \text{Var}(t_5 - t_4) = 8 \text{Var}(t_4); \quad (28)$$

Analogous to (23) this is easily computed as

$$\text{Var}(t_4) = h N_A i \text{Var}(\rho_i) + h \rho_i^2 \text{Var}(N_A); \quad (29)$$

where N_A and ρ_i are defined as in the proof of Lemma 3.1. Thus with $h N_A i = L=2$, $\text{Var}(N_A) = (1 - \rho_1)L=2$ and $h \rho_i^2 i = 1 = \rho_1$, $\text{Var}(\rho_i) = (1 - \rho_1) = \frac{1}{2}$ we get

$$\text{Var}(\rho_1) = 4L \frac{(2 - \rho_1)}{2} \quad (30)$$

Proof of Lemma 3.1. Let $\rho_k > L$. Then the low density region of A particles extends over the whole lattice, and there is only a finite number of B particles (discrepancies) in the system. Therefore an A-jam will form at the right boundary blocking the entrance of B particles, whereas A particles will not be blocked. The number of particles in the A-jam performs a biased random walk increasing on average as explained in the proof of Lemma 3.2, and thus the jam will reach the left boundary in an expected time of order L . At this point the density of A particles on all even sites is 1 and if there are any singular B particles left, they will leave the system in a time of order L and the system reaches a symmetry broken configuration as defined in Section 2.2.

3.3 Proof of Theorem 2

Assume the system to have symmetry broken distribution $\rho_A = \begin{pmatrix} 1 \\ 0 \end{pmatrix}$ as defined in Section 2.2 with particle species B expelled from the system. The density profile of A particles is given by the stationary measure for the single species system which is known exactly [20]. For $L \rightarrow \infty$ this means $\rho_A(i) = 1 + o(1)$ for even sites and $\rho_A(i) = 1 - \frac{1}{2} + o(1)$ for odd sites, up to boundary effects at the left boundary with $i = O(1)$. Species

B is expelled from the system and injection of B particles is only possible if site L is empty. Exact expressions given in [20] (equation (18)) yield

$$P_A(L) = 1 - \frac{(1-q)^L}{(1-q)^L} = 1 - (1-q)^L : \quad (31)$$

Thus the probability that site L is empty is exponentially small in the system size, and the expected time $\langle T_A \rangle$ until the minority species can penetrate the system started in the broken state is exponentially large in L. This is not surprising even without knowledge of the exact expressions, since for injection of the first B particle the complete jam of A particles has to be dissolved against the drive Δ and this jam consists of the order of L particles.

4 Simulation results

4.1 Results for T_1

In the proof of Theorem 1 we identified a bound on the expected number of cycles $\langle k \rangle$ until the amplification loop stops, which is called k in the following. This bound grows like $k(L) = C + \ln L = (2 \ln q)$ with increasing L (18). To estimate the constant C we replace $\langle \sigma_1 \rangle$ in (16) by $\frac{1}{L} \text{Var}(\sigma_1) = 4L \frac{(2-q)^2}{2}$ as given in (11) and get

$$k(L) = \frac{\ln L}{2 \ln q} + 2 + \frac{\ln(2-q)^2}{2 \ln q} : \quad (32)$$

With this choice of C, $k(L)$ is no longer a strict upper bound but in very good agreement with simulation results for $\langle k \rangle$, as can be seen in Figure 4. In particular the simulation data show the same logarithmic growth with prefactor $(2 \ln q)^{-1}$ as $k(L)$, so in this sense the rigorous bound of Theorem 1 is sharp.

As can be seen in Figure 3 (bottom) the number of cycles needed in each realization depends heavily on the initial fluctuation σ_1 , which is a random quantity even in the limit $L \rightarrow \infty$. Thus we do not expect a law of large numbers for k , which is also supported by Figure 4. The bars indicate the standard deviation of the distribution of k which is more or less independent of the system size.

4.2 Stationary results

The stationary dynamics consists mainly of flipping between the two symmetry broken states which are close to ρ_A and ρ_B . We define the flip times

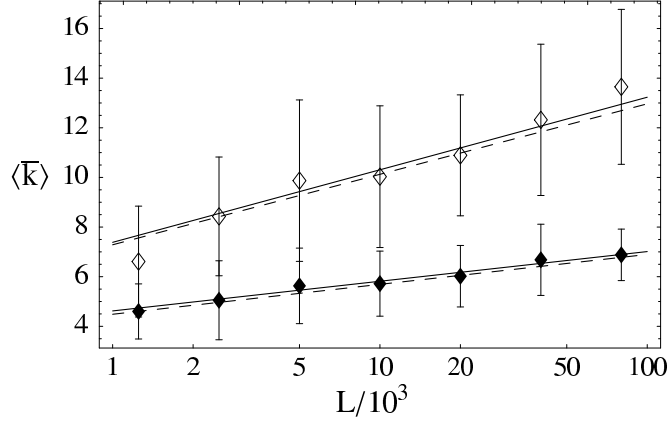


Figure 4: Simulation results for $\langle k \rangle$ for different system sizes L . The data are obtained as averages over 100 realizations, the average values are shown as \diamond for $\beta = 0.5$, \circ for $\beta = 0.4$ and \square for $\beta = 0.9$, \triangle for $\beta = 0.5$. Errors are of the size of the symbols and the bars denote the standard deviations of the distribution of k . The full lines (—) give a linear fit to the data points which agree very well with the estimate $k(L)$ given in (32), shown as dashed lines (---).

to be the times between two consecutive sign changes of $\phi_A - \phi_B$, where $\phi_A = \frac{1}{L} \sum_{i=1}^L \phi_A(i)$ is the (time dependent) number of A particles in the system normalized by L , and ϕ_B is defined analogously. A typical trajectory of $(\phi_A - \phi_B)(t)$ is shown in Figure 5 (upper left), showing that there is a clear timescale of flipping between the two states. The lower left plot of Figure 5 shows simulation data for the cumulative tail of the distribution of the random variable τ . This distribution clearly consists of two parts, one of which are small τ times $\tau = O(1)$ which result from fluctuations during a single transition between the two symmetry broken states. The relevant τ times are the ones that increase with the system size marking the lifetime of the symmetry broken states. In the upper right plot of Figure 5 the average value of these relevant τ times, denoted by $\langle \tau \rangle$ is shown to increase exponentially in the system size as $\langle \tau \rangle \sim z^L$. For $\beta = 0.5$, $\beta = 0.4$ we measure $z = 1.31 \pm 0.02$ and for $\beta = 0.9$, $\beta = 0.5$ $z = 2.55 \pm 0.08$. Both values are larger than β , respectively, consistent with the result (31) for T_2 , which is a lower bound for the relevant τ times. Normalizing the data by $\langle \tau \rangle$ in the lower two plots of Figure 5 results in a data collapse for the extensive part of the distribution. The non-extensive part collapses to a jump at $x = 0$ in the cumulative tail (lower left plot), showing that a substantial fraction of sign changes have τ times of $O(1)$. The lower right shows a logarithmic plot of the tail of the renormalized extensive part

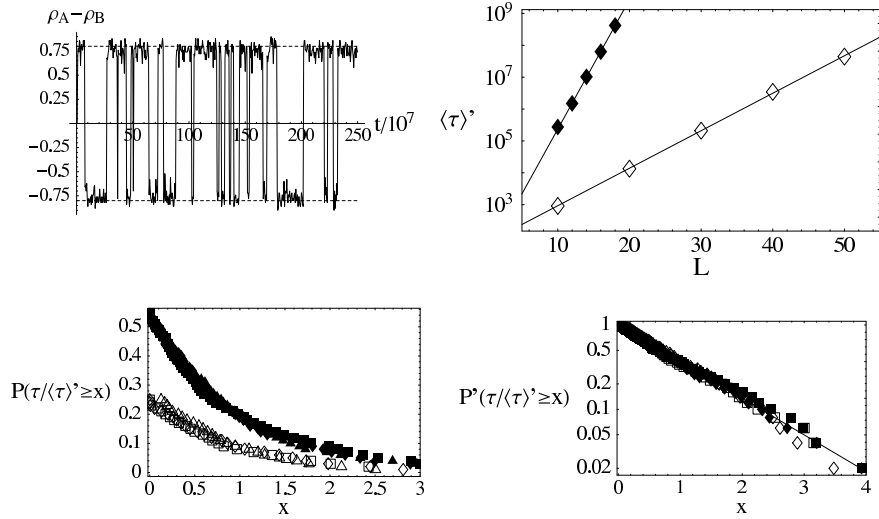


Figure 5: Study of the ip time distribution. The upper left plot shows $\rho_A - \rho_B$ as a function of time for $\rho = 0.5$ and $\rho = 0.4$ and $L = 50$. The other plots show data for $\rho = 0.5$, $\rho = 0.4$ (unfilled symbols) and $\rho = 0.9$, $\rho = 0.5$ (black symbols). The average values of the relevant ip times $\langle \tau \rangle$ (see text) are shown to be exponentially increasing in L in the upper right plot. The full lines give a linear fit to the data points. The lower left shows the cumulative tail of the distribution of normalized ip times $\tau/\langle \tau \rangle$ for $L = 30$ (4), $L = 40$ (), $L = 50$ () and $L = 14$ (N), $L = 16$ (), $L = 18$ (). The same symbols apply in the lower right, a logarithmic plot of the cumulative tail of the renormalized distribution of relevant ip times. The full line denotes an exponential distribution with parameter 1.

of the distribution, i.e. the distribution of relevant ip times (denoted by P^0) showing good agreement with an exponential distribution of parameter 1. Therefore we conclude that the relevant ip times have an exponential distribution, with average value increasing exponentially in L .

5 Dynamics on the transition line

For the borderline case $\rho = \rho_c$ the dynamics of the system can still be effectively described in terms of boundary jams and low density regions. The cyclic behavior can be observed (see Figure 6, upper left), but fluctuations are larger since the end of a jam is dissolving and the cycle lengths, though still of order L , are strongly fluctuating. But according to (24) there is no

amplification of fluctuations during a cycle. Instead, ρ_k is not driven towards L but is diffusing, so a symmetry broken state can still be reached within $O(L^2)$ cycles, and thus $T_1 = O(L^3)$. On the other hand, when the system is in one of the symmetry broken states, the length of the jam of the majority species is only diffusing. So it dissolves in a time of only $T_2 = O(L^2)$, which is the lifetime of a symmetry broken state for $\rho = 0.5$. Thus, no symmetry breaking takes place in this case. Instead, for large L a typical conformation is taken from a cycle, consisting of jams with diffusing length and of low density regions for both species. An average over many realizations leads to an approximately linear stationary density profile as shown in Figure 1 (lower left). Further, for $\rho = 0.5$ site 2 (L) is occupied by A particles for approximately half of a cycle length with probability 0.5 , leading to the stationary densities $\rho_A(2) = 0.5$ and $\rho_A(L) = 0.5$. For odd sites an analogous argument yields $\rho_A(1) = 0$ and $\rho_A(L-1) = 0.5$, which agrees well with Figure 1.

Moreover, the formation and dissolution of boundary jams for the two species shows interesting temporal correlations [11]. In the following we study the distribution of τ times between sign changes of $(\rho_A - \rho_B)(t)$, analogous to the symmetry broken case. In Figure 6 we show three plots of $\rho_A - \rho_B$ against time on different time scales for $\rho = 0.5$. For these parameters the maximal difference, given by the average density in the symmetry broken phase, is given by $1 - 0.5 = 0.5$. In a time of order L^2 the path explores the whole interval $[-0.5; 0.5]$ (see lower right plot), but for smaller time scales the paths show a self-similar structure (see lower left and upper right plot). Therefore one observes τ times on all length scales and in the limit $L \rightarrow \infty$ we expect a scale free distribution of τ . This is confirmed in Figure 7, showing a double logarithmic plot of the cumulative tail $P(\tau > x)$. Data for different system sizes collapse without scaling and show agreement with a power law tail with exponent -0.5 . For large x the data deviate from this behavior, due to boundary effects for smaller values of L as discussed above, and due to numerical inaccuracies, using quantiles to determine the cumulative tail.

The exponent of the power law can be predicted by comparison with a random walk. $L(\rho_A - \rho_B)$, the difference in the number of particles as a function of time performs a symmetric random walk for $\rho = 0.5$ on the interval $[-L; L]$. Thus we use the scaling ansatz $P(\tau > x) \sim L^{-\alpha} g(x/L^2)$. The argument $x = L^2$ follows from the scaling of first passage times of symmetric random walks in one dimension and the fact that τ is the return time to the origin. The power α can be fixed by the requirement that $h_i = O(L)$, since the average return time to 0 is inversely proportional to the stationary distribution at 0. This scales as $1/L$ because the stationary distribution of

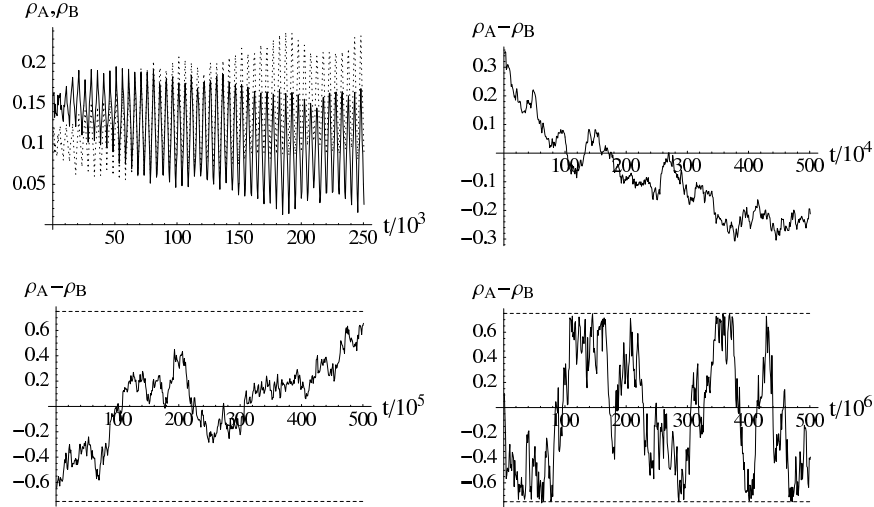


Figure 6: Density profiles for $\alpha = 0.5$ on different time scales. The upper left plot shows ρ_A (full line) and ρ_B (dashed line). The other plots show the difference $\rho_A - \rho_B$. The plots are stationary samples and do not start at $t=0$, the axes only indicate the time scale.

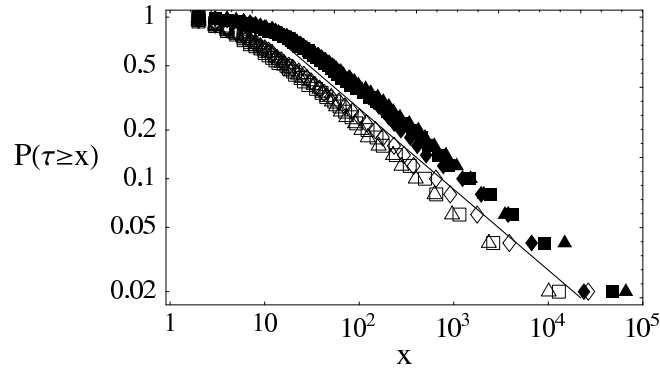


Figure 7: Double logarithmic plot of the cumulative tail of the distribution of waiting times. Data for $\alpha = 0.9$ are shown as $N(L=3200)$, $L=6400$, $L=12800$, corresponding unfilled symbols for $\alpha = 0.5$. The full line indicates the inclination of a power law exponent 0.5.

the random walker is a linear function on $[L; L]$. We get

$$h i \int_0^{L^{-1}} L^{-2} g(x=L^2) \frac{dx}{L^2} = O(L^{-2}) ; \quad (33)$$

and thus $\beta = 1$ and a consistent ansatz is

$$P(\tau > x) = L^{-1} g(x=L^2) ; \quad (34)$$

To cancel the L -dependence for $L \rightarrow 1$ we have $g(y) = 1 - \frac{p}{y}$ as $y \rightarrow 0$ for the scaling function and thus for x large enough

$$P(\tau > x) = 1 - \frac{p}{x} \quad \text{for } x \ll L^2 ; \quad (35)$$

giving the observed exponent 0.5 .

6 Conclusion

In the present article we investigated spontaneous symmetry breaking (SSB) in a two-species driven cellular automaton model with deterministic bulk behavior and stochastic open boundary conditions. We analyzed in detail the dynamical mechanisms leading to SSB. Its main feature is a cyclic amplification of initial fluctuations taking a time of order $L \ln L$, while a traffic jam phenomenon keeps the system in a SSB state for an exponentially large time. This lead to a proof of SSB in the thermodynamic limit using a simple martingale argument without further assumptions on the rates, and to rigorous asymptotic estimates for the relevant time scales in the broken phase. The above mechanism is very different from the freezing-by-cooling scenario for broken ergodicity in one-component systems [4] that results from a localization of shocks [21, 22, 23].

Some dynamical and stationary properties at the phase transition line have been predicted analytically (but not rigorously) in terms of boundary jams and low density regions using the picture developed for the discussion of the broken phase. In particular, we found an asymptotically scale-free distribution of ip times between sign changes in the difference of particle numbers. The decay exponent of the distribution has been predicted using random walk arguments and confirmed by numerical simulations. The exact phase transition line can be predicted correctly by a mean-field approximation. The density profiles predicted in this way, however, differ from the numerically computed density profiles [19]. Therefore mean-field theory is unreliable at the phase transition line, and was not presented in this paper, whereas the correct density profiles could be predicted in Section 5 by a rather simple argument.

The amplification mechanism outlined above does not apply in the symmetric phase $\phi < \phi_c$ since the formation of boundary jams, a key ingredient for the amplification, does not work. The length of a boundary jam is driven towards small values so the boundary sites are not blocked and particles are injected all the time. It is an intriguing open question whether similar mechanisms are at work in the original bridge model of [1, 2].

Acknowledgments

We thank M. R. Evans and V. Popkov for useful discussions. S.G. and G.M.S. are grateful for the hospitality of the Isaac Newton Institute for Mathematical Sciences, where part of this work has been carried out.

References

- [1] M. R. Evans, D. P. Foster, C. Godreche and D. Mukamel, Spontaneous Symmetry Breaking in a One Dimensional Driven Diffusive System, *Phys. Rev. Lett.* 74 (2) 208-211 (1995).
- [2] M. R. Evans, D. P. Foster, C. Godreche and D. Mukamel, A symmetric exclusion model with two species: Spontaneous symmetry breaking, *J. Stat. Phys.* 80 :69-102 (1995).
- [3] C. Godreche, J.M. Luck, M. R. Evans, D. Mukamel, S. Sandow and E.R. Speer, Spontaneous symmetry breaking: exact results for a biased random walk model of an exclusion process, *J. Phys. A* 28 (21) :6039-6071 (1995).
- [4] A. Rakos, M. Paessens and G.M. Schutz, Hysteresis in one-dimensional reaction-diffusion systems, *Phys. Rev. Lett.* 91 238302 (2003).
- [5] E. Levine and R.D. Williams, Spontaneous Symmetry Breaking in a Non-Conserving Two-Species Driven Model, *J. Phys. A* 37 :3333-3352 (2004).
- [6] P.F. Amdt, T. Heinzel and V. Rittenberg, First-Order Phase Transitions in One-Dimensional Steady States, *J. Stat. Phys.* 90 :783-815 (1998).
- [7] M. Cliney, M. R. Evans and D. Mukamel, Symmetry breaking through a sequence of transitions in a driven diffusive system, *J. Phys. A* 34 : 9923-9937 (2001).
- [8] D.W. Erickson, G. Pruessner, B. Schmittmann and R.K.P. Zia, Spurious phase in a model for traffic on a bridge *J. Phys. A* 38 (41): L659-L665 (2005).

- [9] E. Pronina and A.B. Kolomeisky, Spontaneous Symmetry Breaking in Two-Channel Asymmetric Exclusion Processes with Narrow Entrances, *cond-mat/0611472*.
- [10] V. Popkov and G.M. Schutz, Why spontaneous symmetry breaking disappears in a bridge system with PDE-friendly boundaries, *J. Stat. Mech.: Theor. Exp.*, P12004 (2004).
- [11] V. Popkov, Infinite reflections of shock fronts in driven diffusive systems with two species, *J. Phys. A* 37 (5):1545-1557 (2004).
- [12] V. Popkov and G.M. Schutz, Shocks and excitation dynamics in a driven diffusive two-channel system, *J. Stat. Phys.* 112:523-540 (2003).
- [13] B. Toth and B. Valko, Onsager relations and Eulerian hydrodynamics for systems with several conservation laws *J. Stat. Phys.* 112 (3-4): 497-521 (2003).
- [14] M. Cliney, B. Derrida, M.R. Evans, Phase transition in the ABC model, *Phys. Rev. E* 67 (6):066115 (2003).
- [15] V. Popkov, M. Salerno, Hydrodynamic limit of multichain driven diffusive models, *Phys. Rev. E* 69 (4):046103 (2004).
- [16] J. Fritz and B. Toth, Derivation of the Leroux system as the hydrodynamic limit of a two-component lattice gas, *Comm. Math. Phys.* 249 (1):1-27 (2004).
- [17] B. Toth, B. Valko, Perturbation of singular equilibria of hyperbolic two-component systems: a universal hydrodynamic limit, *Comm. Math. Phys.* 256 (1):111-157 (2005).
- [18] G.M. Schutz, Critical phenomena and universal dynamics in one-dimensional driven diffusive systems with two species of particles *J. Phys. A* 36 R339-R379 (2003).
- [19] R.D. Williams, G.M. Schutz, S. Grobksky, Dynamical origin of spontaneous symmetry breaking in a field-driven nonequilibrium system, *Europhys. Lett.* 71 (4):542-548 (2005).
- [20] Schutz G., Time-dependent correlation functions in a one-dimensional asymmetric exclusion process, *Phys. Rev. E* 47 (6):4265-4277 (1993).
- [21] A. Parmeggiani, T. Franosch and E. Frey, Phase coexistence in driven one-dimensional transport, *Phys. Rev. Lett.* 90 (8):086601 (2003).

- [22] V. Popkov, A. Rakos, R.D. Willmann, A.B. Kolomeisky and G.M. Schutz, Localization of shocks in driven diffusive systems without particle number conservation, *Phys. Rev. E* 67 (6):066117 (2003).
- [23] M.R. Evans, R. Juhasz and L. Santen, Shock formation in an exclusion process with creation and annihilation, *Phys. Rev. E* 68:026117 (2003).